12-2012

Quantified H I morphology : VI. The morphology of extended discs in UV and H I.

Benne W. Holwerda
University of Louisville

N. Pirzkal
Space Telescope Science Institute

J. S. Heiner
Universidad Nacional Autonoma de Mexico

Original Publication Information

Holwerda, B. W., N. Pirzkal and J. S. Heiner. "Quantified H I Morphology - VI. The Morphology of Extended Discs in UV and H I." 2012. *Monthly Notices of the Royal Astronomical Society* 427(4): 3159-3175.

Monthly Notices
of the
ROYAL ASTRONOMICAL SOCIETY

Mon. Not. R. Astron. Soc. **427,** 3159–3175 (2012) doi:10.1111/j.1365-2966.2012.21975.x

Quantified H I morphology – VI. The morphology of extended discs in UV and H I

B. W. Holwerda,[1⋆] N. Pirzkal[2] and J. S. Heiner[3]

[1] *European Space Agency, ESTEC, Keplerlaan 1, 2200 AG, Noordwijk, the Netherlands*
[2] *Space Telescope Science Institute, Baltimore, MD 21218, USA*
[3] *Centro de Radiastronomía y Astrofísica, Universidad Nacional Autónoma de México, 58190 Morelia, Michoacán, Mexico*

Accepted 2012 August 22. Received 2012 August 22; in original form 2012 March 2

ABSTRACT

Extended ultraviolet (XUV) discs have been found in a substantial fraction of late-type – S0, spiral and irregular – galaxies. Similarly, most late-type spirals have an extended gas disc, observable in the 21-cm radio line (H I). The morphology of galaxies can be quantified well using a series of scale-invariant parameters; concentration-asymmetry-smoothness (CAS), Gini, M_{20}, and G_M parameters. In this series of papers, we apply these to H I column density maps to identify mergers and interactions, lopsidedness and now XUV discs.

In this paper, we compare the quantified morphology and effective radius (R_{50}) of the Westerbork observations of neutral Hydrogen in Irregular and SPiral galaxies Project (WHISP) H I maps to those of far- and near-ultraviolet images obtained with *GALEX*, to explore how close the morphology and scales of H I and UV in these discs correlate. We find that XUV discs do not stand out by their effective radii in UV or H I. However, the concentration index in far-ultraviolet (FUV) appears to select some XUV discs. And known XUV discs can be identified via a criterion using asymmetry and M_{20}; 80 per cent of XUV discs are included but with 55 per cent contamination. This translates into 61 candidate XUV disc out of our 266 galaxies, 23 per cent consistent with previous findings. Otherwise, the UV and H I morphology parameters do not appear closely related.

Our motivation is to identify XUV discs and their origin. We consider three scenarios; tidal features from major mergers, the typical extended H I disc is a photo-dissociation product of the XUV regions and both H I and UV features originate in cold flows fueling the main galaxy.

We define extended H I and UV discs based on their concentration ($C_{\rm HI} > 5$ and $C_{\rm FUV} > 4$ respectively), but that these two subsamples never overlap in the WHISP sample. This appears to discount a simple photo-dissociation origin of the outer H I disc.

Previously, we identified the morphology space occupied by ongoing major mergers. Known XUV discs rarely reside in the merger-dominated part of H I morphology space but those that do are type 1. The exceptions, XUV discs in ongoing mergers, include the previously identified UGC 4862 and UGC 7081, 7651, and 7853. This suggests cold flows as the origin for the XUV complexes and their surrounding H I structures.

Key words: galaxies: interactions – galaxies: ISM – galaxies: spiral – galaxies: star formation – galaxies: statistics – galaxies: structure.

1 INTRODUCTION

The interest in the outskirts of spiral galaxy discs has increased over recent years as these regions are the site of the most recent acquisition of gas for these systems (e.g. Sancisi et al. 2008), as well as low-level star formation (e.g. Dong et al. 2008; Bigiel et al. 2010a; Alberts et al. 2011, for recent results), making these faint outskirts the interface between the island universes – the galaxies themselves – and the cosmic web of primordial gas.

The low-level star formation was first discovered in Hα emission by Ferguson et al. (1998) and Lelièvre & Roy (2000). After the launch of the *Galaxy Evolution EXplorer* (*GALEX*, Martin et al. 2005), initial anecdotal evidence pointed to ultraviolet discs of spiral

⋆E-mail: benne.holwerda@esa.int

galaxies extending much beyond their optical radius (Thilker et al. 2005b,a; Gil de Paz et al. 2005, 2007b; Zaritsky & Christlein 2007). Subsequent structural searches for these extended ultraviolet (XUV) discs by Thilker et al. (2007) and Lemonias et al. (2011) find that some 20–30 per cent of spirals posses an XUV disc and 40 per cent of S0s (Moffett et al. 2012), making this type of disc common but not typical for spiral and S0 galaxies. These XUV disc complexes are generally ∼100 Myr old, explaining why most lack Hα (Alberts et al. 2011), as opposed to a top-light initial mass function (IMF) (as proposed by Meurer et al. 2009), and sub-solar but not excessively low metallicities (Gil de Paz et al. 2007b; Bresolin et al. 2009; Werk et al. 2010, 0.1–1 $Z_{\odot}$, based on emission lines). Additionally, it has been known for some time now that atomic hydrogen (H I) as observed by the 21 cm fine structure line also extends well beyond the optical disc of spiral galaxies (e.g. Begeman 1989; Meurer et al. 1996; Meurer, Staveley-Smith & Killeen 1998; Swaters et al. 2002a; Noordermeer et al. 2005a; Walter et al. 2008; Boomsma et al. 2008; Elson, de Blok & Kraan-Korteweg 2011; Heald et al. 2011b,a; Zschaechner et al. 2011). In those few cases where both high-quality H I and deep *GALEX* data are available, a close relation in their respective morphology was remarked upon (Bigiel et al. 2010a). While we have to wait for the all-sky surveys in H I to catch up to the coverage of the *GALEX* surveys (e.g. the wide survey with WSRT/APERTIF or the WALLABY survey with ASKAP), we can compare the morphology for those galaxies for which uniform H I information is available.

The canonical view of the origin of the XUV discs is that the Kennicutt–Schmidt law (Kennicutt 1998) needs to be extended to low global surface densities of gas and the formation of individual O-stars in the very outskirts of discs (Cuillandre et al. 2001; Bigiel et al. 2010b). The recent accretion of cold gas flows (Kereš et al. 2005) into the H I disc is the origin for the young stars (the fueling rate implied by XUV discs is explored in Lemonias et al. 2011) and H I warps (Roškar et al. 2010). The fraction of spirals that have an XUV disc (∼20–30 per cent) supports this scenario as the remaining spirals may simply have no current cool gas inflow. In this case, one would expect UV and H I morphology to follow each other reasonably closely for the XUV discs but not for many of the others, as the star formation in the inner disc is more closely related to the molecular phase (Bigiel et al. 2008). However, the existence of XUV discs pose an intriguing alternate possibility for the origin of the atomic hydrogen disc. Instead of primordial gas accreting on to the disc, the H I disc could also be the by-product of photo-dissociation of molecular hydrogen on the 'skins' of molecular clouds by the ultraviolet flux of the young stars in the XUV disc (see Allen et al. 1997; Allen 2002; Allen, Heaton & Kaufman 2004). This explanation has been explored in the stellar discs of several nearby galaxies (Heiner et al. 2008a,b; Heiner, Allen & van der Kruit 2009, 2010). Gil de Paz et al. (2007b) calculate the time-scales (molecular gas dissociation and re-formation) involved but these are inconclusive regarding the origin of the XUV disc. In this scenario, one would expect the UV and H I morphologies to follow each other closely in all cases; in the outer disc, the UV flux from a few young stars would reach out to large areas of the low-column density gas to dissociate enough hydrogen to form the outer H I disc. Thus, the low-flux and low-H I column density morphology – those defining the limits and extent of the XUV and H I discs – should show a close relation in parameters such as concentration, Gini, M_{20} and the effective radius. A third explanation is in terms of recent tidal interaction. A major merger often pulls gas out of the planes of galaxies and triggers star-forming events. Some anecdotal evidence (e.g. UGC 04862 is a late-stage major merger Torres-Flores et al. 2012) does point to this possible origin. In this scenario, one would expect that most H I discs hosting an XUV disc would be seriously tidally disrupted.

In this series of papers, we have explored the quantified morphology of available H I maps with the common parameters for visible morphology; concentration-asymmetry-smoothness, Gini and M_{20} and G_M. In Holwerda et al. (2011c), we compare the H I morphology to other wavelengths, noting that the H I and ultraviolet morphologies are closely related. In subsequent papers of the series, we use the H I morphology to identify mergers (Holwerda et al. 2011d), their visibility time (Holwerda et al. 2011a) and subsequently infer a merger rate from WHISP (Westerbork observations of neutral Hydrogen in Irregular and Spiral galaxies Project; Holwerda et al. 2011b), as well as identify phenomena unique to cluster members (Holwerda et al. 2011e).

In this paper, we explore the morphological link between the H I and XUV discs in WHISP (van der Hulst, van Albada & Sancisi 2001; van der Hulst 2002), a survey of several hundred H I observations of nearby galaxies. We complement this data with *GALEX* images to explore the morphology and typical scales of these maps. A direct and quantified comparison between the gas and ongoing star-formation morphology could help answer open questions regarding the origin and nature of XUV discs: how do their respective sizes relate? Are their morphologies closely related in every case? Do their respective morphologies point to a dominant formation mechanism; gas accretion, photo-dissociation or tidal? Are XUV discs in morphologically distinct or typical H I discs? Are XUV discs embedded in H I discs that appear to be in an active interaction? What is the relation between UV flux and H I column density in the XUV discs, especially the outer disc?

The paper is organized as follows; Section 2 gives the definitions of the quantified morphology parameters we employ, and Section 3 describes the origin the data. We describe the application of the morphological parameters and the results in Sections 4 and 5, and we discuss them in Section 6. We list our conclusions and discuss possible future work in Section 7.

2 MORPHOLOGICAL PARAMETERS

In this series of papers, we use the concentration–asymmetry–smoothness parameters (CAS, Conselice 2003), combined with the Gini-M_{20} parameters from Lotz, Primack & Madau (2004) and one addition of our own: G_M. We have discussed the definitions of these parameters in the previous papers, as well as how we estimate uncertainties for each. Here, we will give a brief overview but for details we refer the reader to Holwerda et al. (2011c,d).

We select pixels in an image as belonging to the galaxy based on the outer H I contour and adopt the position from the 2MASS catalogue (Kleinmann et al. 1994) as the central position of the galaxy. Given a set of n pixels in each object, iterating over pixel i with value I_i, position x_i, y_i with the centre of the object at x_c, y_c these parameters are defined as

$$C = 5\log(r_{80}/r_{20}), \tag{1}$$

with r_f as the radial aperture, centred on x_c, y_c containing percentage f of the light of the galaxy (see definitions of r_f in Bertin & Arnouts 1996; Holwerda 2005).[1] We include the r_{50}, or 'effective radius' in

[1] We must note that the earlier version of our code contained an error, artificially inflating the concentration values. A check revealed this to be $C_{\rm new} = 0.38C_{\rm old}$, and we adopt the new, correct values in this paper.

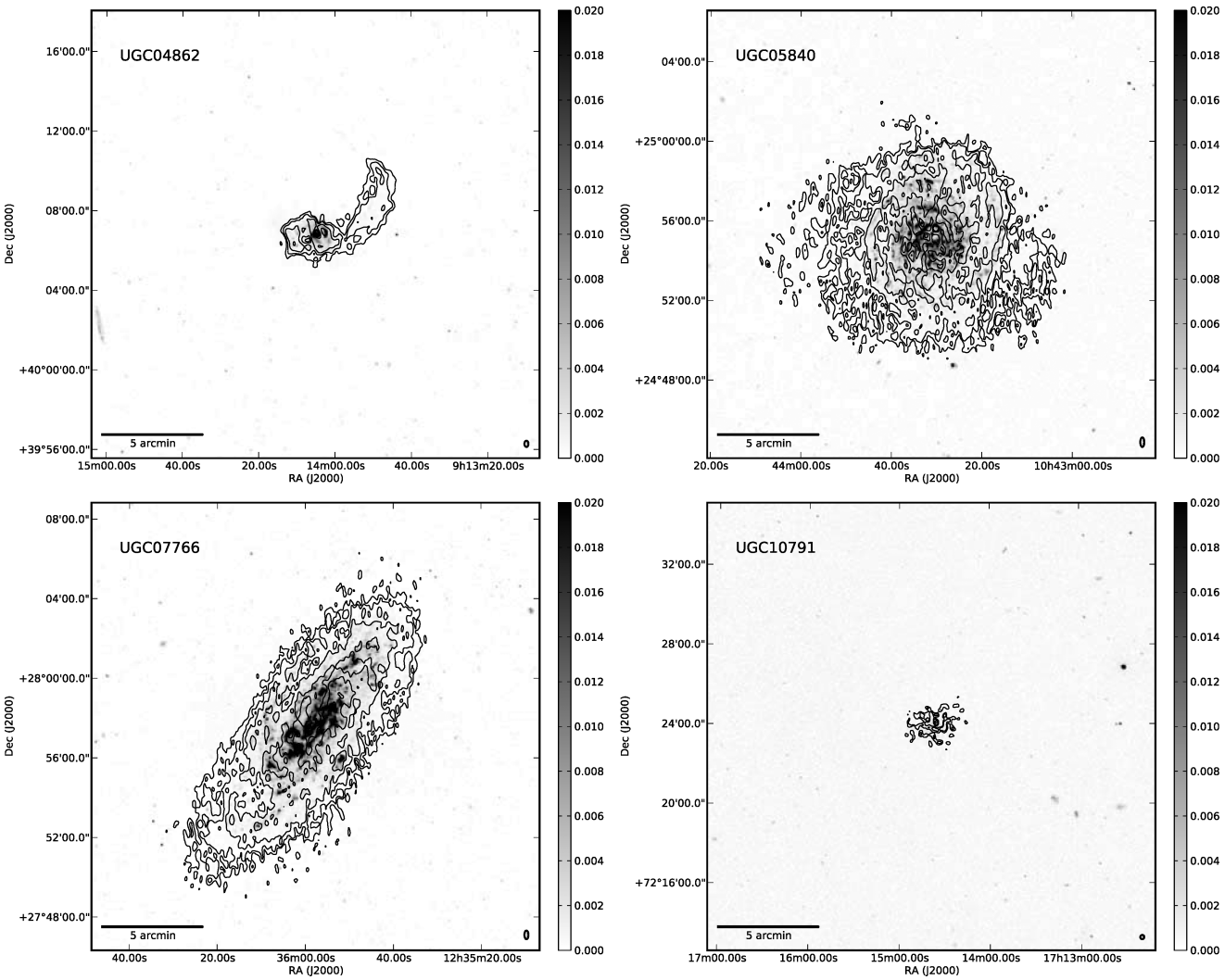

Figure 1. The few examples of XUV discs, type 1 (individual UV complexes) as classified by Thilker et al. (2007) with complementary H I data in WHISP. The tidal feature in UGC 04862 is studied in detail by Torres-Flores et al. (2012), who report high metallicities and 1–11 Myr ages for the UV complexes. They speculate that their origin is either from the galaxies that formed UGC 04862 or that the current star formation is a later generation enriched system.

our catalogue as well:

$$A = \frac{\Sigma_i |I_i - I_{180}|}{\Sigma_i |I(i)|}, \tag{2}$$

where I_{180} is the pixel at position i in the galaxy's image, after it was rotated 180° around the centre of the galaxy, and

$$S = \frac{\Sigma_{i,j} |I(i,j) - I_S(i,j)|}{\Sigma_{i,j} |I(i,j)|}, \tag{3}$$

where I_S is pixel i in a smoothed image. The type of smoothing (e.g. boxcar or Gaussian) has changed over the years. We chose a fixed 5 arcsec Gaussian smoothing kernel for simplicity.

The Gini coefficient is defined as

$$G = \frac{1}{\bar{I} n(n-1)} \Sigma_i (2\mathrm{i} - n - 1) I_i, \tag{4}$$

where the list of n pixels was first ordered according to value and $\bar{I}$ is the mean pixel value in the image,

$$M_{20} = \log \left(\frac{\Sigma_i M_i}{M_{tot}} \right), \quad \text{for } \Sigma_i I_i < 0.2 I_{\rm tot}, \tag{5}$$

where M_i is the second-order moment of pixel i; $M_i = I_i\ [(x - x_c)^2 + (y - y_c)^2]$. $M_{\rm tot}$ is the second-order moment summed over all pixels in the object and M_{20} is the relative contribution of the brightest 20 per cent of the pixels in the object. Instead of using the intensity of pixel i, the Gini parameter can be defined using the second-order moment:

$$G_M = \frac{1}{\bar{M} n(n-1)} \Sigma_i (2\mathrm{i} - n - 1) M_i. \tag{6}$$

These parameters trace different structural characteristics of a galaxy's image but these do not span an orthogonal parameter space (see also the discussion in Scarlata et al. 2007).

3 DATA

We use three data sets for this paper; H I radio observations from WHISP or The H I Nearby Galaxy Survey (THINGS), and ultraviolet observations from *GALEX* space telescope observations.

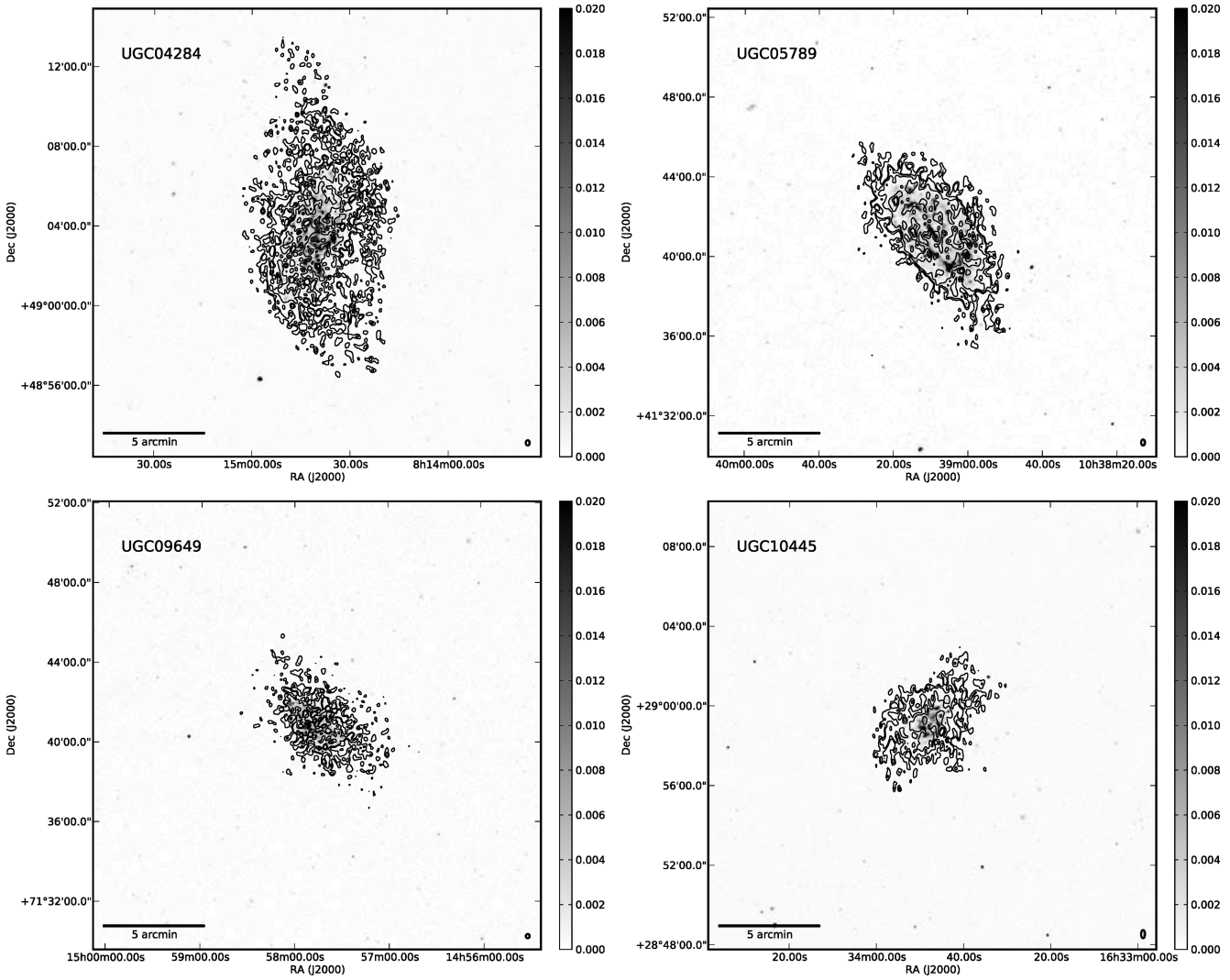

Figure 2. The two known examples of type 2 XUV discs, a ring of UV outside the optical disc (top) and the two examples of type 1/2, a combination of types 1 and 2, as classified by Thilker et al. (2007), which are also in the WHISP sample. The H I morphology is remarkably flocculant and lacks grand spiral structure.

3.1 WHISP Sample

The starting data set here is the 266 observations done as part of WHISP (van der Hulst et al. 2001; van der Hulst 2002, 339 individual galaxies) that also have reasonable quality far-ultraviolet (FUV) and near-ultraviolet (NUV) data. The WHISP observation targets were selected from the Uppsala General Catalogue of Galaxies (Nilson 1973), with blue major axis diameters >2.0 arcmin, declination (B1950) >20° and flux densities at 21 cm larger than 100 mJy, later lowered to 20 mJy. Observation times were typically 12 h of integration. The galaxies satisfying these selection criteria generally have redshifts less than 20 000 km s^{-1} ($z < 0.07$). WHISP has mapped the distribution and velocity structure of H I in several hundreds of nearby galaxies, increasing the number of H I observations of galaxies by an order of magnitude. The WHISP project provides a uniform data base of data cubes, zeroth-order and velocity maps. Its focus has been on the structure of the dark matter halo as a function of Hubble type, the Tully–Fisher relation and the dark matter content of dwarf galaxies (Swaters et al. 2002b; Swaters & Balcells 2002; Noordermeer et al. 2005b; Zwaan et al. 2005). Until the large all-sky surveys with new instruments are completed, WHISP is the largest, publicly available data set of resolved H I observations.[2] We compiled a catalogue of basic data (position, radial velocity etc.) (see for details Holwerda et al. 2011b).

3.1.1 H I data

We use the highest available resolution zero-moment maps (beam size of ∼12 arcsec × 12/sin(δ)), from the WOW website and converted these to $M_\odot$ pc^{-2} column density maps with J2000 coordinates and of the same size as the *GALEX* postage stamp (see for details Holwerda et al. 2011b).

3.1.2 GALEX data

To complement the H I column density maps, we retrieved *GALEX* (Martin et al. 2005) postage stamps from http://skyview.gsfc.nasa.gov, near- and far-ultraviolet (1350–1750

[2] Available at 'Westerbork On the Web' (WOW) project at ASTRON (http://www.astron.nl/wow/).

and 1750–2750 Å). The majority of observations were taken as part of the AIS, MIS, NGS, etc. imaging surveys and hence vary in depth and signal-to-noise. Spatial resolution is 4–6 arcsec, depending on position in the field-of-view.

Of the 339 galaxies in WHISP, 266 had reliable FUV information and this cross-section is what we use for the remainder of the paper. The FUV images with H I contours overlaid are shown in Figs 1 and 2, and Figs A1 and A2 (see Supporting Information with the online version of the article), and for all galaxies in Appendix C (see Supporting Information).

3.1.3 XUV classifications

In the WHISP sample, Thilker et al. (2007) classified 22 galaxies for the presence and type of XUV discs. The type 1 XUV discs are characterized by discrete regions out to high radii and type 2 by an anomalously large, UV-bright outer zone of low optical surface brightness. Table 1 lists the XUV classifications for the WHISP sample; 22 from Thilker et al. (2007) and a single one from Lemonias et al. (2011). The latter study's lack of overlap is unsurprising as they focus on a more distant sample in complement to the Thilker et al.'s nearby sample ($D < 40$ Mpc). We designate an XUV disc with both a type 1 and type 2 as type 1/2 to discriminate in the plots below and mark those galaxies in WHISP surveyed by Thilker et al. that do not have an XUV disc as type 0.

Figs 1 and 2 show the overlap between WHISP and the XUV discs identified by Thilker. The type 1 collection includes a single merger remnant (UGC 4862) and some H I discs that appear slightly lopsided, tentatively supporting a tidal origin as one path to generate type 1 discs. Fig. 3 shows the H I contours around those WHISP galaxies inspected by Thilker et al. but not found to contain an XUV disc. There are two instances of clear ongoing mergers as well as a variety of H I morphologies.

Table 1. XUV discs classified by Thilker et al. (2007) and one from Lemonias et al. (2011) for the WHISP galaxies in their respective samples.

Name	UGC	Type
–	1913	0
–	4165	0
–	4274	0
–	4273	0
NGC 2541	4284	2
–	4325	0
–	4499	0
NGC 2782	4862	1
–	5556	0
NGC 3319	5789	2
NGC 3344	5840	1
–	6856	0
–	7323	0
NGC 4258	7353	1
–	7651	0
NGC 4559	7766	1
–	7853	0
NGC 4625	7861	1
NGC 5832	9649	1/2
–	10445	1/2
–	10791	1
–	12754	0

3.2 THINGS

Since the overlap between the WHISP sample and the Thilker et al. XUV classification sample is small, we also compare the THINGS survey's H I and FUV morphologies to their classifications of XUV discs (Table 2). We use the morphological information from Holwerda et al. (2011c), with the concentration definition appropriately amended. The morphological classifications are based on the public data sets from THINGS (Walter et al. 2008),[3] and *GALEX* Nearby Galaxy Atlas (NGA, Gil de Paz et al. 2007a),[4] retrieved from MAST (http://galex.stsci.edu). We use the robust-weighted (RO) THINGS column density maps as these are similar in resolution as the native resolution of *GALEX* for the contour of 0.3×10^{20} cm^{-2}, approximately the spatial extent of the H I disc. Table 2 lists the THINGS galaxies that have XUV disc classifications from Thilker et al. (2007). The benefits of the THINGS sample are that there is an XUV classification for all galaxies, the H I and UV data are of comparable spatial resolution, and the *GALEX* observations are of uniform depth. The drawbacks are that it is an equally small sample as the WHISP overlap and that there is only a single ongoing merger in this sample as it was constructed to be quiescent.

4 APPLICATION OF QUANTIFIED MORPHOLOGY TO H I AND *GALEX* DATA

Before we compute the quantified morphology parameters described above, we preprocess the images as follows. First, we cut out a postage stamp of both the H I maps and *GALEX* data centred on the UGC position. Similar to Holwerda et al. (2011b), we use a stamp size of 22×22 arcmin around this position. We then smooth the *GALEX* data to approximately the same spatial resolution as the WHISP H I data ($\sim$12 arcsec). We use the H I map to define the part of the data over which the morphological parameters are computed over in the same manner as in Holwerda et al. (2011b,d); a threshold of 10^{20} atoms cm^{-2}.

We then compute the above quantified morphology parameters for the H I map and FUV, and NUV images (summarized in Tables C1, C3 and C2, full versions available as Supporting Information with the online version of the article). In addition to the above parameters, we compute the effective or half-light radius (R_{50}) for each image as an indication of disc size on the sky.

5 ANALYSIS

To explore in what type of H I disc XUV discs predominantly occur, we first compare the relative effective radii of the H I and UV discs, secondly compare the individual morphological parameters in both H I and UV against one another, and thirdly explore the UV and H I morphologies alone, to explore if XUV can be identified from UV morphology and to see if XUV discs are predominantly in merging or interacting discs.

5.1 Effective radii

First we compare the relative sizes of the NUV and FUV discs and the H I disc through their effective radii, the radius which contains 50 per cent of the total flux. A naive expectation would be that in the case of extended UV discs, these would be similar to the H I

[3] http://www.mpia-hd.mpg.de/THINGS/
[4] http://galex.stsci.edu/GR4/

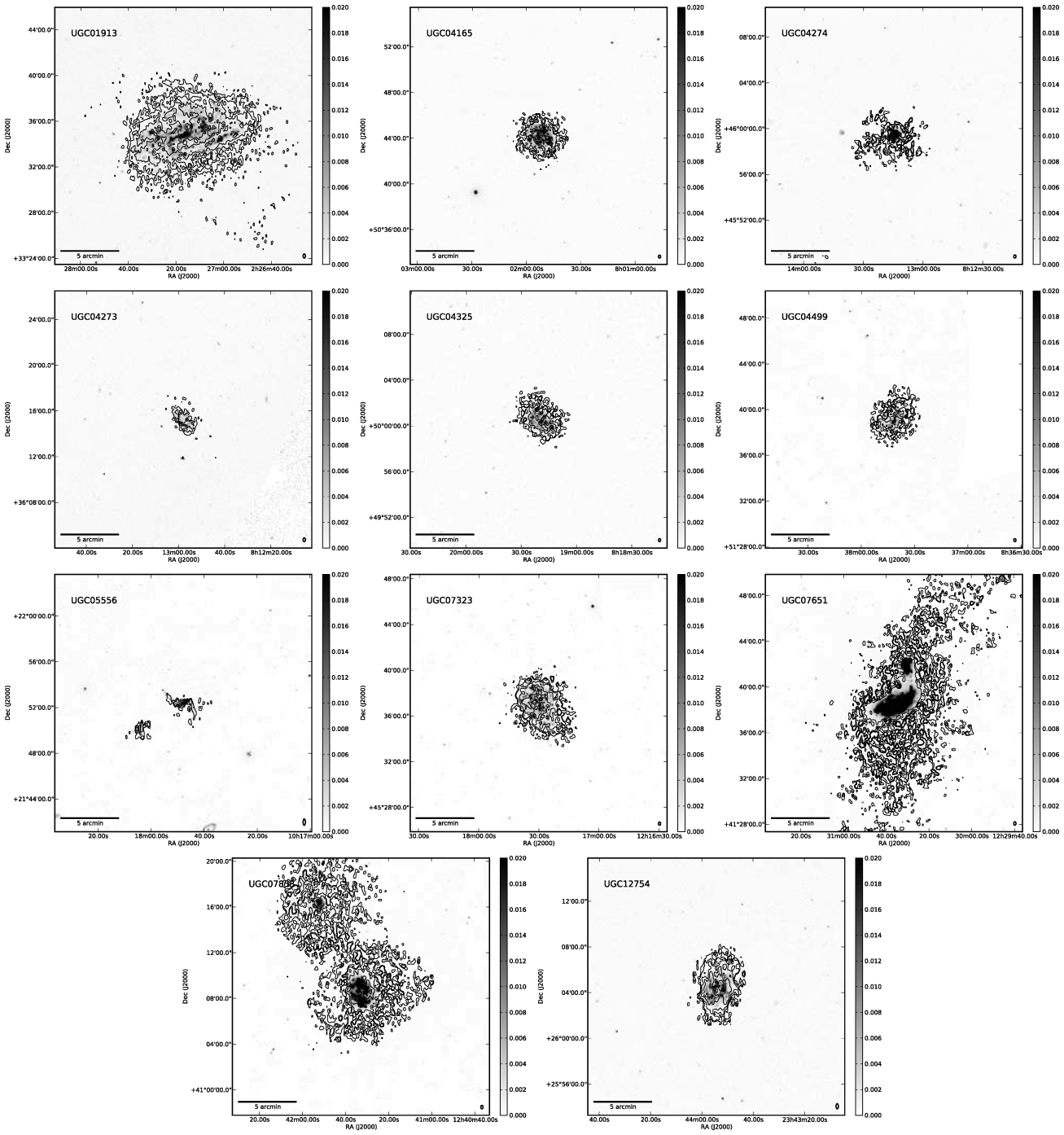

Figure 3. The type 0 XUV discs – no XUV disc identified by Thilker et al. (2007) – in the WHISP sample. There are two ongoing major mergers as well as a range of H I morphologies.

values. Fig. 4 shows the ratio of the effective radii ($R_{\rm eff}$) for H I and FUV or NUV. Neither ratio singles out those identified by Thilker et al. (2007) as extended UV discs. Thus the ratio of effective radii is not a good metric to automatically select XUV discs.

5.2 UV versus H I morphologies

Figs 5 and 6 show the concentration, asymmetry, smoothness, Gini, M_{20} and the G_M of the NUV and FUV compared to their values in the H I maps, as computed over the same area and convolved to the same spatial resolution. We note that our approach is different from that of Lemonias et al. (2011) who use the *optical* concentration to identify the approximate galaxy type.

Concentration of the UV and the H I shows two distinct sets of outliers. One where the UV concentration is more than 3; these are relatively extended discs. Some of the XUV discs from Thilker et al. (2007) can be found here, but by no means all; two type 1/2 and one type 1 is not. However, six of the non-XUV discs are also above the $C_{\rm FUV} > 4$ line. Figs 7 and 8 show that most type 1 in the THINGS sample are here. The other set of outliers have H I concentration

Table 2. XUV discs classified by Thilker et al. (2007) for those THINGS galaxies in their sample.

Name	Type	Reference
NGC 628	1	Lelièvre & Roy (2000) Alberts et al. (2011)
NGC 925	0	
NGC 2403	1/2	
Holmberg-II	0	
M81A	0	
DDO53	0	
NGC 2841	1	Alberts et al. (2011)
NGC 2903	0	
HolmbergI	0	
NGC 2976	0	
NGC 3031	1	
NGC 3184	0	
NGC 3198	1	
IC2574	2	
NGC 3351	0	
NGC 3521	0	
NGC 3621	1	Alberts et al. (2011)
NGC 3627	0	
NGC 4736	0	Zaritsky & Christlein (2007)
DDO154	0	
NGC 4826	0	
NGC 5055	1	Alberts et al. (2011)
NGC 5194	0	
NGC 5457	1	
NGC 6946	0	
NGC 7331	0	
NGC 7793	0	

indices exceeding $C_{\rm HI} > 5$. However, these are not necessarily the classical H I discs which extend well outside the stellar disc. High concentration values such as these often indicate recent tidal activity (Holwerda et al. 2011d). We will use the concentration indices in FUV and H I to set our own supplementary definition of an extended disc; XUV$_c$ discs are defined by $C_{\rm FUV} > 4$ and extended H I discs (XH I) by $C_{\rm HI} > 5$ in the other plots. We do so to identify these outliers in the other plots to explore their nature, not to supplant the original detailed classification by Thilker et. al. The XUV$_c$ discs have UV flux distributed throughout their otherwise unremarkable H I disc and XHI discs are extended in H I but not special in UV. If we compare the ratio of concentration indices in Fig. 9 for the WHISP galaxies, both the XUV$_c$ and XHI discs – unsurprisingly – stand out very clearly. This is confirmed by the ratios of THINGS concentration index in Fig. 10. We note, however, that if one applies these criteria blindly to the THINGS data (dashed lines in Fig. 8), one would conclude that most THINGS galaxies are XUV$_c$ discs. Morphological criteria such as these need to be recalibrated when applied to different quality data.

XUV and XUV$_c$ discs have much lower values of the M_{20} parameter in the UV than the general WHISP population. There is a general trend between M_{20} and concentration (specifically for the 3.6 μm Spitzer images; Muñoz-Mateos et al. 2009; Holwerda et al., in preparation), so extreme values for this parameter are not surprising as such, especially if identified with a concentration criterion (see also Fig. 11). The *lower* value of M_{20} implies that regions that make up the XUV disc do not contribute to the brightest 20 per cent of all the pixels in these UV images; the general UV flux is more extended and hence the second-order moment is less concentrated in the brightest few regions. The H I M_{20} values however are quite within the normal range of WHISP galaxies. Thus, perhaps the UV M_{20} values offer an alternative automated definition of XUV discs in combination with concentration.

The XUV discs show a median value for asymmetry in FUV, but the full range in H I.

In UV smoothness, the XUV discs do not stand well apart from the general WHISP population. In the case of the G and G_M parameters, XUV discs avoid extreme values for the UV and generally fall below the G_M(H I) = 0.6 criterion for interactions. In the case of most of the H I morphological parameters, the values for the XUV discs are typical for the bulk of WHISP galaxies.

Based on their relative H I and UV morphologies, the previously identified or automatically identified XUV discs mostly stand out in their UV concentration and M_{20} values. In the remaining UV parameters and all H I morphological values, they appear to be mixed in with the bulk of the WHISP (Figs 5 and 6) and THINGS (Figs 7 and 8).

5.3 XUV disc UV morphology

In this section we look at the UV morphological parameters in detail to explore if bona fide XUV discs can be identified from their UV morphology alone – as computed over an area defined by the H I disc. For this we can use the 22 galaxies in WHISP and the THINGS sample, both classified by Thilker et al.

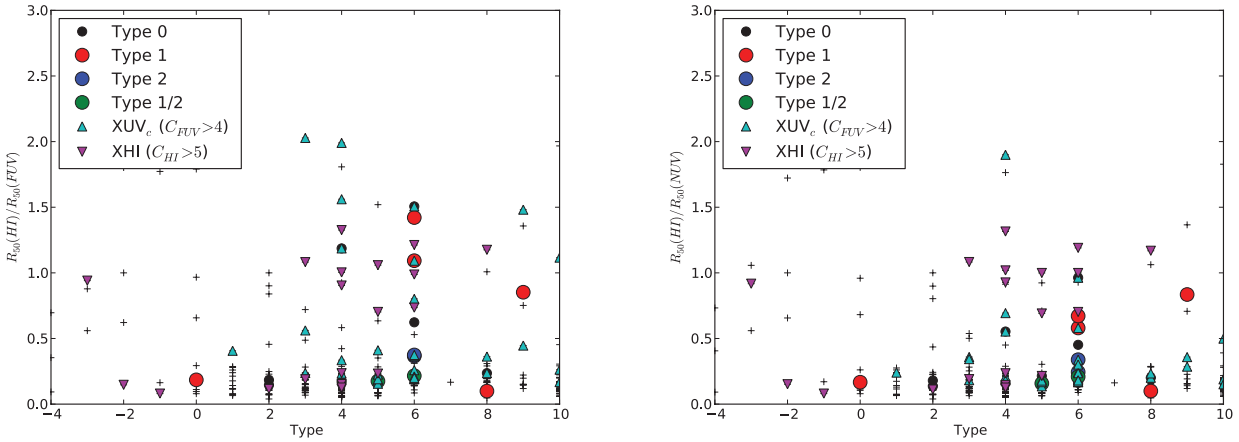

Figure 4. The ratio of effective radii (R_{50}) of the H I over UV as a function of Hubble type as a function of type.

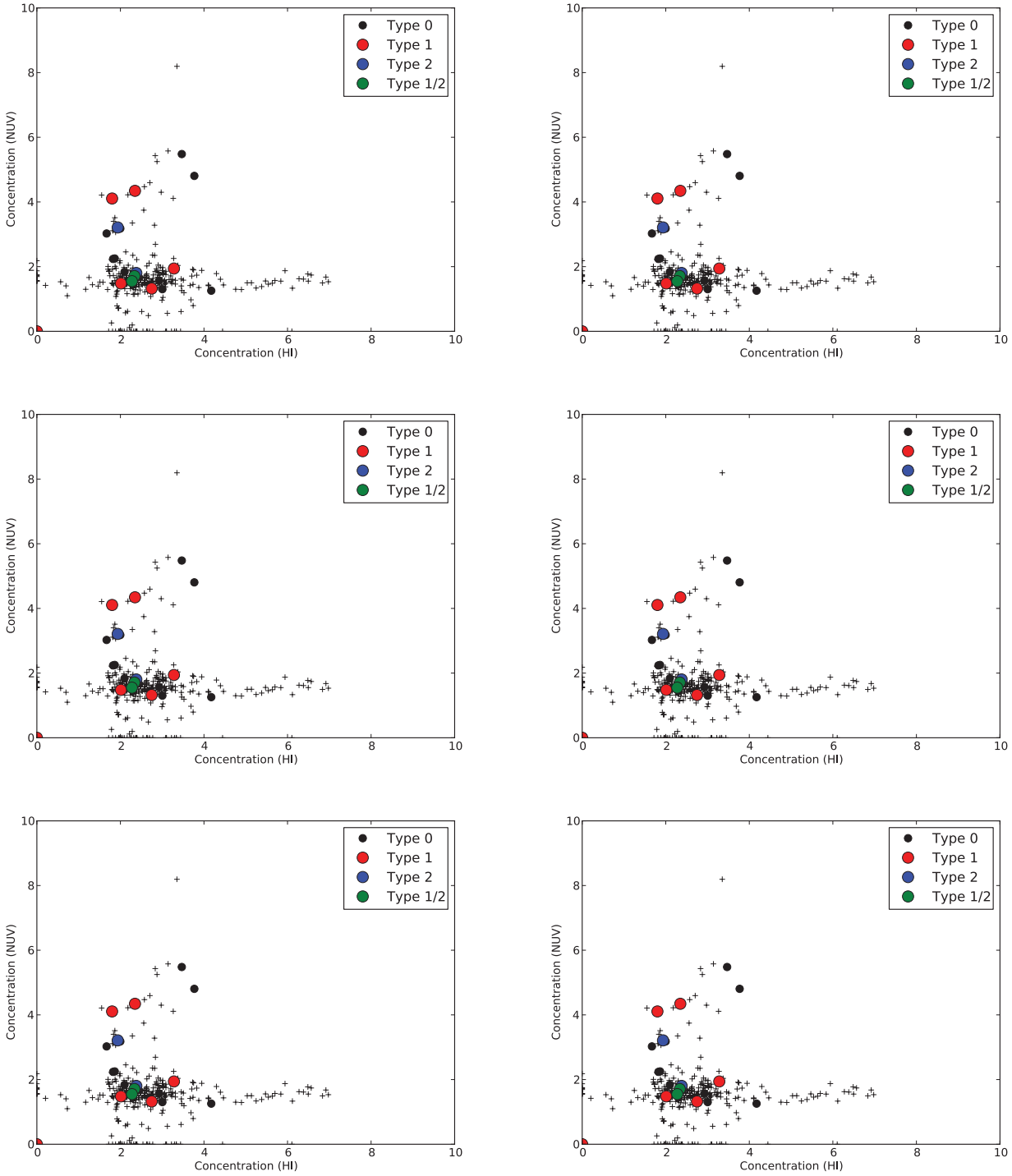

Figure 5. The morphological parameters of the H I disc and NUV data; concentration (C), asymmetry (A), smoothness (S), the Gini index (G), and the second-order moment of the brightest 20 per cent of the pixels (M_{20}), and the Gini index of the second-order moment (G_M).

Fig. 11 shows the FUV parameters for the XUV discs identified by Thilker et al. (2007) as well as those discs inspected but without an extended UV component for both samples.

The above concentration-only criterion (XUV$_c$, $C_{\rm FUV} > 4$) preselects a number of the XUV discs but it would miss several bona fide XUV discs as well as include many false positives. Using the information in two (or possibly more) parameters is how we identify mergers and may identify (candidate) XUV discs. On inspection of the distributions of the NUV and FUV parameters (Figs B2 and B3 in the Supporting Information), there are several combinations of parameters that offer the possibility of pre-selecting XUV discs without too much loss: Gini-asymmetry, M_{20}-asymmetry and Gini-G_M. The goal is not to just select only the bona fide, previously identified XUV discs but also to exclude as many discs, that were previously classified as non-XUV as practical. This latter criterion immediately excludes Gini–asymmetry and Gini–G_M combinations. The combination of M_{20} and asymmetry in FUV is promising and we define the following criterion to identify XUV

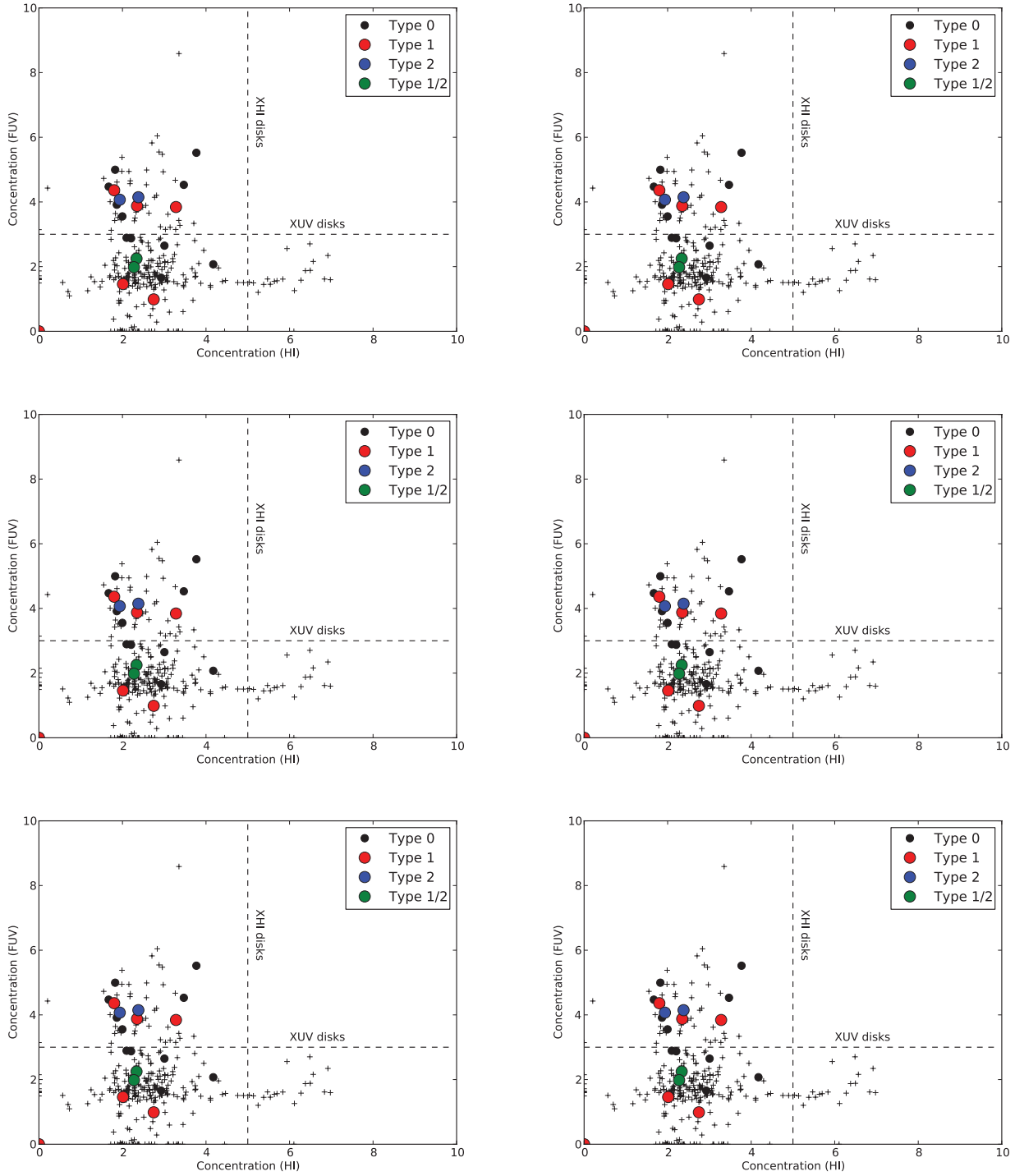

Figure 6. The morphological parameters of the H I disc and FUV data; concentration (C), asymmetry (A), smoothness (S), the Gini index (G), and the second-order moment of the brightest 20 per cent of the pixels (M_{20}), and the Gini index of the second-order moment (G_M).

discs in an FUV survey (6 arcsec resolution):

$$|A - (-0.27M_{20} + 0.12)| < 0.14, \quad (7)$$

which works well for the THINGS sample and we divide the linear relation by a factor 2 for the WHISP survey (to account for the ∼12 arcsec resolution):

$$|A - (-0.27M_{20} + 0.12)/2| < 0.14. \quad (8)$$

Both are illustrated in Fig. 11 with dashed lines. Table 3 lists the two criteria – the simple concentration criterion and the M_{20}-asymmetry one (adjusted for each survey) – and their success rate (percentage of all bona fide XUV discs included) and contamination rate (percentage of all classified objects that are non-XUV). The M_{20}-asymmetry criterion selects most XUV but with a contamination of some 55 per cent of non-XUV discs. A future search for XUV discs could therefore use this as a first cut before visual classification. Given the 109 WHISP galaxies selected by this criterion (Table A1, see

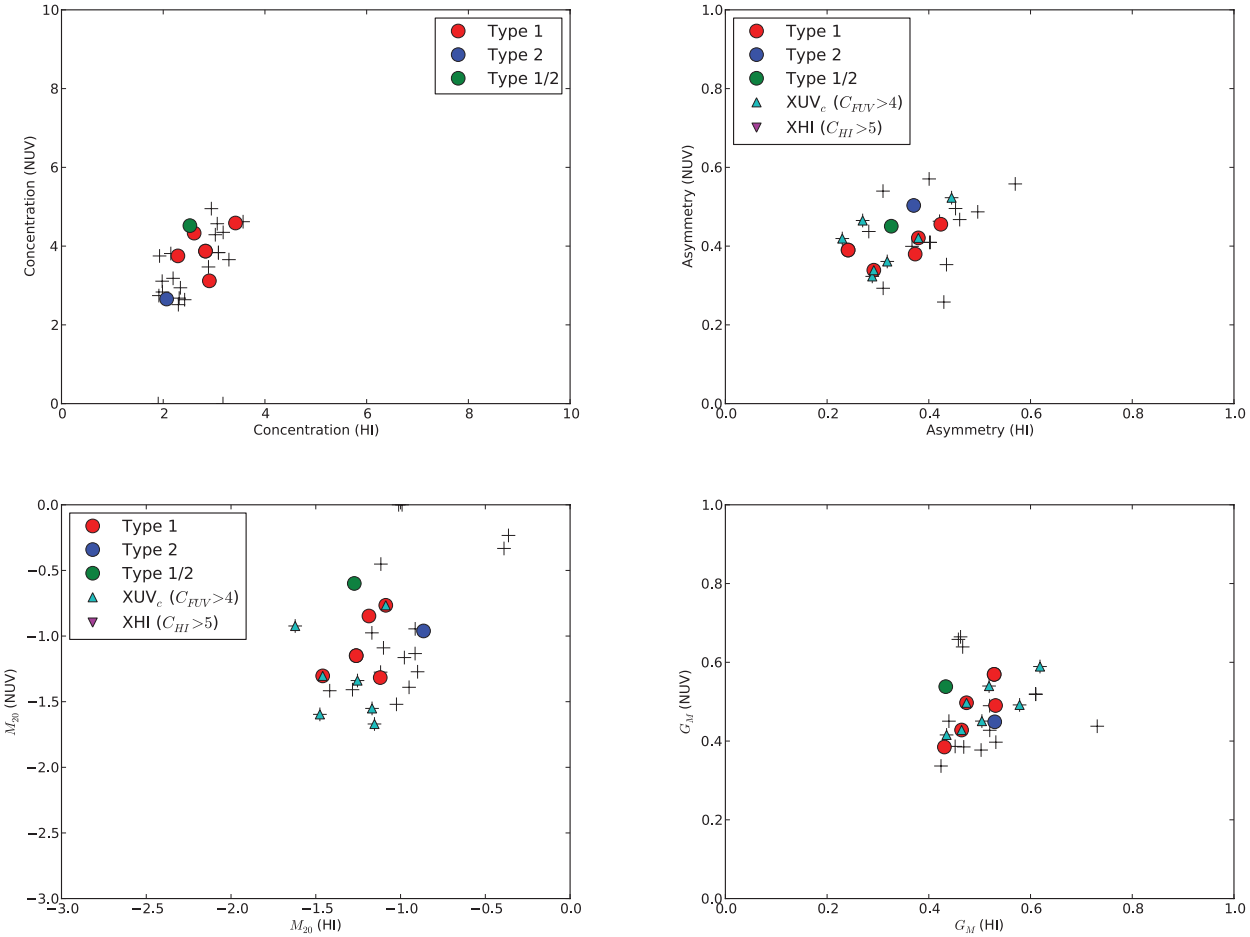

Figure 7. The morphological parameters of the H I disc and NUV for the THINGS galaxies with the XUV disc classification from Thilker et al. (2007).

the Supporting Information), 61 of these should be bona fide XUV discs, 23 per cent of our sample of 266.

5.4 Are XUV discs in interacting H I discs?

Fig. 12 shows five of the morphological criteria we used or defined in Holwerda et al. (2011a) to identify those discs that are currently undergoing an interaction (see Fig. A1 in the Supporting Information for a similar plot to Fig. 5 in Holwerda et al. (2011d) for a direct comparison). We mark those galaxies identified by Thilker et al. (2007) and those identified as extended UV or H I discs by the concentration parameters.

Based on the H I morphologies, the G_M and C–M_{20} criteria, those H I discs that host an XUV disc are not interacting in the majority of cases. In the case of the other morphological criteria (A–G, A–M_{20}, G–M_{20}), this distinction is not as clear but XUV discs – either selected by Thilker et al. or by their concentration – appear to reside in morphologically very typical H I discs.

At the same time, extended H I discs are often interacting. This is in part because our definition of an interaction is based on concentration, but even in the G_M criterion these are conspicuously separated from the bulk of the H I discs. Typically, the bona fide XUV discs selected by an H I morphological selection of an ongoing merger appear to be type 1, consistent with the first impression from Figs 1 and 2. Thus, mergers appear to be one avenue to generate a type 1 XUV disc.

If we plot these – as a sense check – for the THINGS sample, the XUV discs identified by Thilker et al. (2007) equally appear not to be interacting based on the G_M criterion, but several are based on G–A or M_{20}–G criteria. Several of the non-XUV discs are interactions in A–M_{20}. These criteria would need to be adjusted for the higher resolution of the THINGS sample (difficult to do without many mergers in the THINGS sample, as we noted in Holwerda et al. 2011c).

6 DISCUSSION

Our first motivation for this study was to explore the possibility if XUV discs could be reliably found using the morphological parameters in UV and H I, especially when computed over a wide aperture such as the H I disc. Based on their morphology parameters in UV and H I, XUV discs identified in Thilker et al. (2007) rarely stand out from the bulk of the WHISP sample, with the exception of M_{20}-A and concentration in UV. In the FUV, the M_{20}-A relation appears reasonably successful in identifying XUV discs and the rate in the WHISP sample (23 per cent) is consistent with the Thilker et al. (2007) and Lemonias et al. (2011) results, for a survey of late-types such as WHISP. The FUV values of asymmetry and M_{20} could therefore be used to identify candidate XUV discs in the local Universe with *GALEX* or similar quality UV data or in deep rest-frame UV observations with *HST*. However, these will have to be computed over a much larger area than commonly used (e.g. the de Vaucouleur diameter D_{25} or the Petrosian radius),

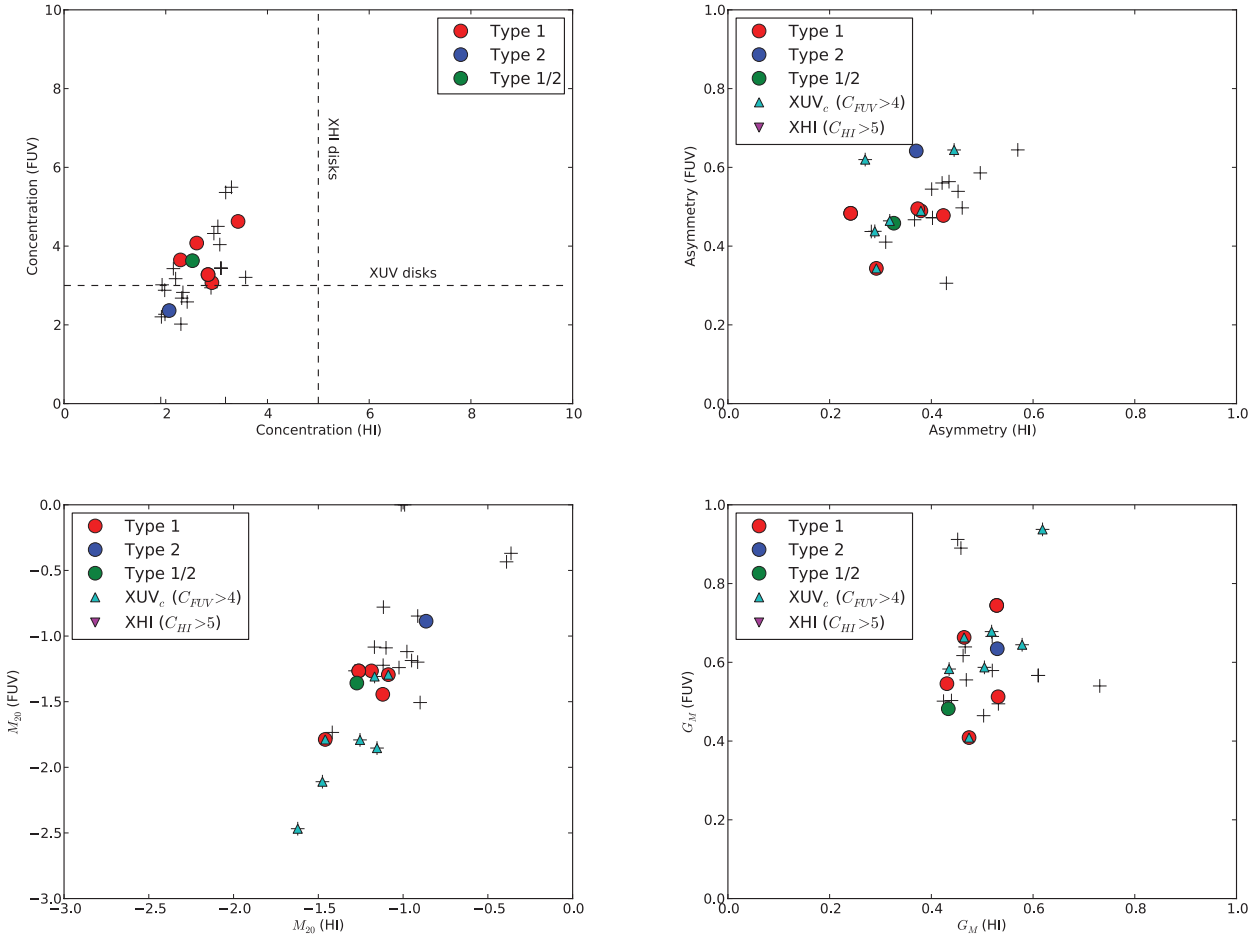

Figure 8. The morphological parameters of the H I disc and FUV for the THINGS galaxies with the XUV disc classification from Thilker et al. (2007). Dashed lines are the H I and UV concentration criteria from Fig. 6.

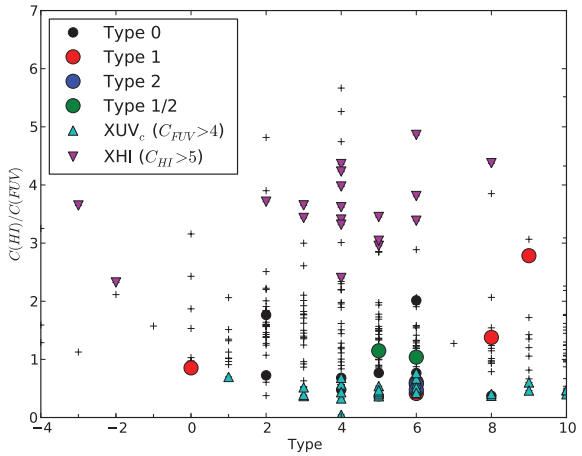

Figure 9. The ratio of concentration in H I over that in UV as a function of Hubble type. In this case (as expected), the XUV and XHI discs stand out.

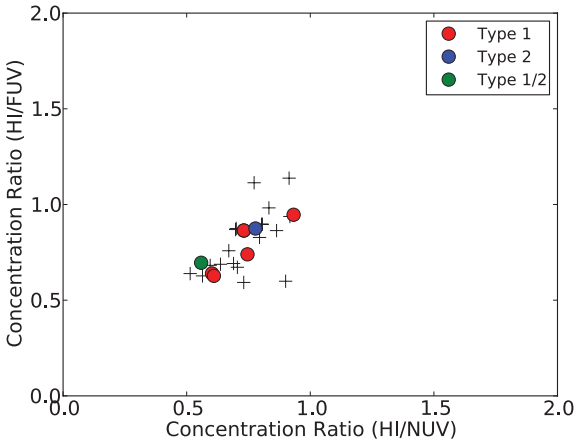

Figure 10. The ratio of concentration of the H I over UV (NUV and FUV) for the THINGS galaxies

such as the one defined by the outer H I contour. The quantified H I and UV morphologies do not correlate as closely as they did for the THINGS sample in Holwerda et al. (2011c) (their Fig. 6). In our opinion, this is due to the wider range of environments probed by the WHISP survey as well as its lower resolution compared to THINGS. A closer relation may return for the inner stellar disc and possibly at higher spatial resolution.

Our second motivation for this work on XUV discs was to explore their origin. Are they the (by)product of (a) cold flow accretion or (b) a gravitational interaction or mergers with another galaxy, or (c) is photo-dissociation of molecular clouds by the UV regions of the XUV discs responsible for the H I discs?

The fact that the majority of the XUV discs do not reside in morphologically distinct H I discs (Figs 6 and 8), precludes the

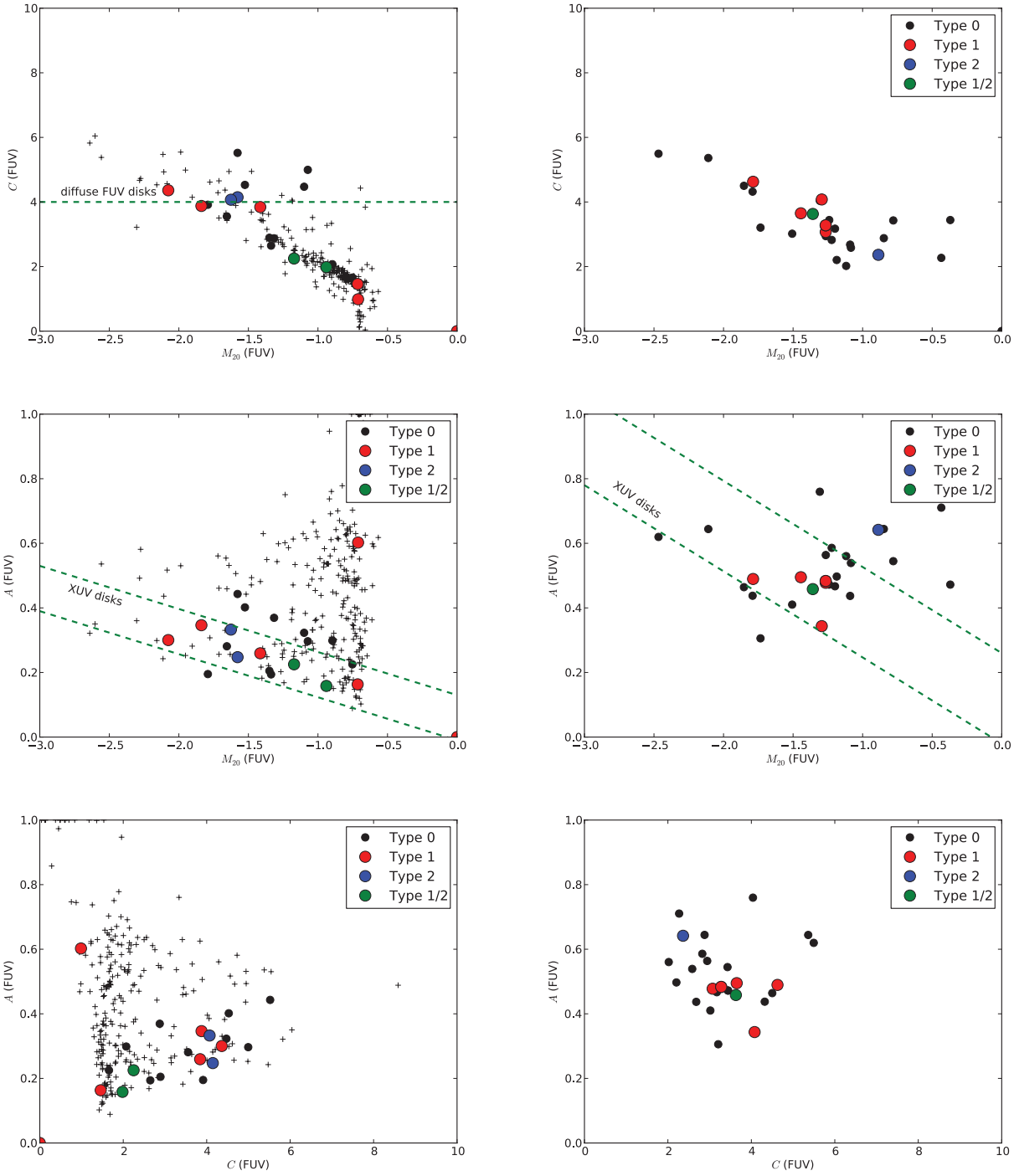

Figure 11. Concentration, asymmetry and M_{20} in FUV for the WHISP (left) and THINGS (right) samples with the Thilker et al. classifications marked. $C_{\rm FUV} > 4$ does not select cleanly the XUV discs previously identified by Thilker et al. The M_{20}-asymmetry criteria (green dashed lines in the middle panels) do select a relatively clean sample of XUV discs from both WHISP and THINGS.

notion that most XUV discs originate from major interaction between galaxies. Few are selected by the previously defined interaction criteria for H I discs. There are, however, some obvious exceptions (Fig. 1). So our naive interpretation for the origin of type 1 discs in Fig. 1 is only partly supported by H I morphology and only holds for type 1.

Since extended UV (XUV$_c$) and extended H I disc (XHI) populations – as defined by their concentration parameter computed over the *same* area – do not coincide (Fig. 6, top left panel), a direct link, such as the photo-dissociation origin of the H I disc, appears less likely. A closer UV–H I relation in morphology may well still hold within the inner stellar disc, especially since the photo-dissociation scenario was developed to explain the higher column densities of H I in this environment (Allen et al. 1997, 2004; Heiner et al. 2008a,b, 2009, 2010). However, the existence of both the $C_{\rm FUV} > 4$ discs without complementary extended H I discs as well as extended ($C_{\rm HI} > 4$) H I discs without a complementary XUV disc appears to be contradictory to the photo-dissociation origin of

Table 3. XUV disc selection criteria and their success (percentage of all bona fide XUV discs included) and contamination rate ('Cont'; percentage of included objects that are non-XUV):

Criterion	WHISP			THINGS	
	XUV (per cent)	Cont (per cent)	Nr	XUV (per cent)	Cont (per cent)
$C_{\rm FUV} > 4$	30.	57	31	25	71
$\lvert A - (- 0.26667 \times M_{20}) + 0.12)/2\rvert < 0.14$	80	55	109	–	–
$\lvert A - (- 0.26667 \times M_{20}) + 0.12)\rvert < 0.14$	–	–	–	87	56

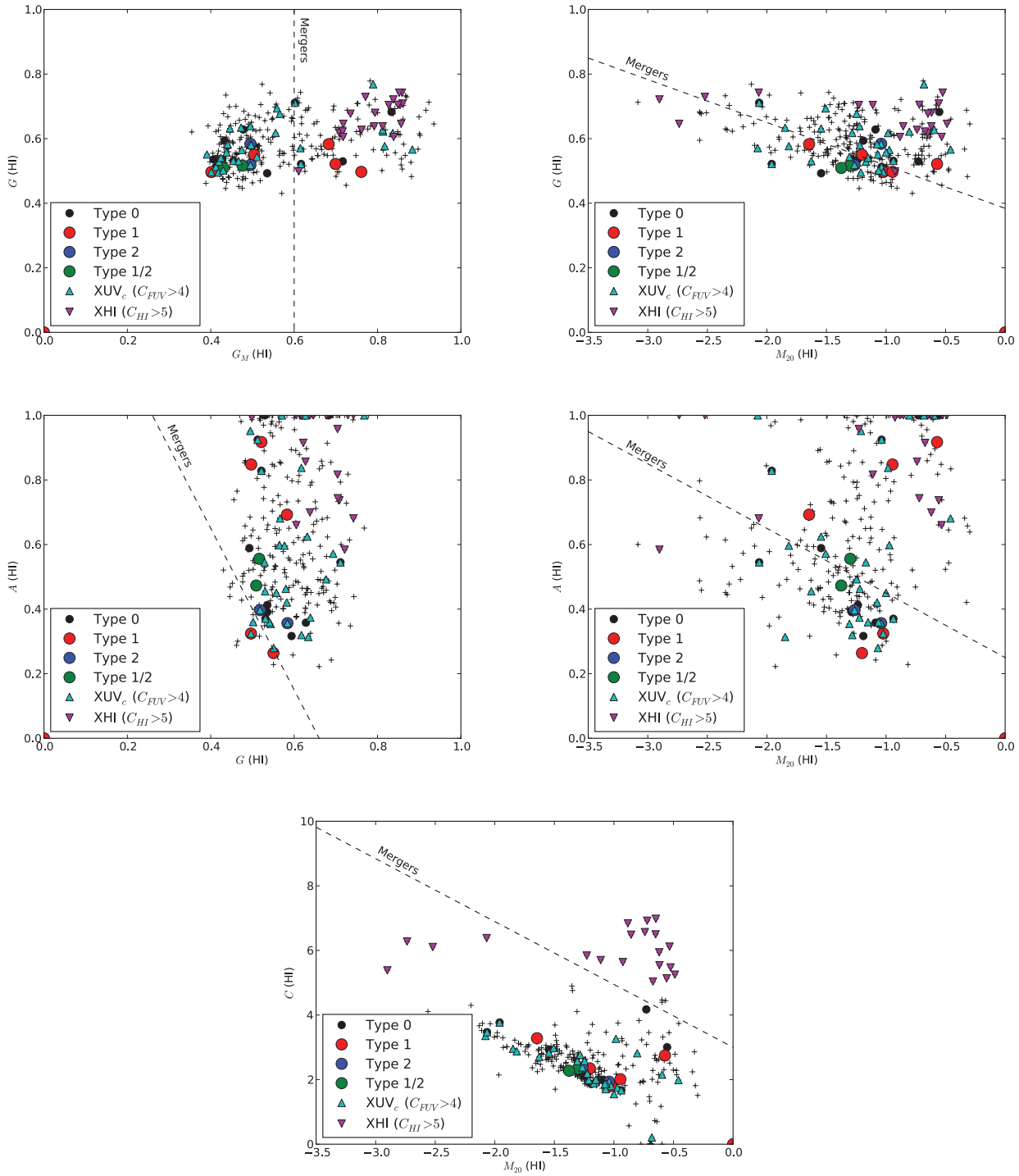

Figure 12. The morphological selection criteria (dashed lines) for H I applied to the WHISP sample. Discs are interactions above and to the right of the dashed lines. XUV discs identified either by Thilker et al. or high FUV or H I concentration are marked.

XHI discs. Two considerations are still in its favour; however, Goggarten et al. (2009) showed that UV emission does not fully trace the lower-level star formation in the low column density environments of the outer disc. Thus, the ionizing stars may be lower-mass main-sequence stars and simply remain undetected in *GALEX* imaging due to their extreme low surface brightness. Also, with higher resolution and more sensitive H I and UV imaging, a closer relation may still return in their quantified morphology (witness the THINGS sample). Thus, we cannot completely rule out a photo-dissociation scenario explaining the relation between H I and UV discs. Similarly, Gil de Paz et al. (2007b) find their time-scale argument for a photo-dissociation origin of XUV discs to be inconclusive.

This leaves cold flows as a likely origin for most XUV discs. A number of these type 1 XUV discs may be the result of a later-stage full merger such as UGC 04862, but judging from the H I morphologies, this is a small fraction of the full XUV or XUV_c sample. Cold flows occur as both a steady trickle along a filament of the Cosmic Web and a discrete accretion in the form of the cold gas originally associated with a small satellite.

There are indirect signs that cold flows are indeed the most common cause for XUV discs. For example, at least three of the nine THINGS galaxies with an XUV disc (M83, NGC 4736 and NGC 5055) are currently cannibalizing a small companion (Martínez-Delgado et al. 2010). Satellites embedded in the gas filament are one of two fueling mechanisms of cold flow; discrete and trickle cold flows (Kereš et al. 2005). The acquired cold gas accompanying the cannibalized companion is a likely trigger for the formation UV complexes. Similarly, those discs selected by their extended UV emission (Fig. A1 in the Supporting Information), often appear to have flocculent, low-column density H I morphologies, which *may* point to recent cold accretion. A few cases (UGC 7081, 7651 and 7853) are obviously interacting major mergers with accompanying H I/UV tidal features. In contrast, the XHI discs are nearly always small galaxies with an obvious close companion (Fig. A2, see Supporting Information), which makes a tidal origin likely for their very extended H I disc.

The quantified morphologies of the WHISP H I and UV discs are not conclusive evidence that cold flows are responsible for the XUV complexes but certainly suggest this is the most likely origin for most, with a few exception due to major interactions.

7 CONCLUSIONS

Based on the quantified morphology of the H I and UV maps of the WHISP sample of galaxies, we conclude the following:

(1) There are distinct galaxy populations that stand out by their high concentration values in FUV or H I (XUV_c and XHI thoughout the paper). These population do not overlap. Some known XUV discs are in the XUV_c sample (Figs 6a, 6e, 8a and 8c).To compute this concentration index, the outer H I contour is needed to delineate the extent of the disc.

(2) The fact that relative dilute UV discs ($C_{\rm FUV} > 4$) and H I discs ($C_{\rm HI} > 5$) population do not overlap at all and the lack of close morphological relations in any other parameters together suggest that a common small-scale origin for the UV and H I discs, such as a photo-dissociation of molecular hydrogen scenario, is less likely for XUV discs (but may still very much hold for the inner discs).

(3) Asymmetry and M_{20} can be used in combination to select XUV discs with reasonable reliability (80 per cent included) but substantial contamination (55 per cent), when properly calibrated for the survey's spatial resolution (equations 7 and 8) and the morphologies are computed over a large enough aperture. With this selection, one can find the number of XUV discs in a survey or candidates for visual classification (Fig. 11).

(4) Based on the morphology of the H I disc in which they occur, XUV discs appear not to occur often in tidally disturbed gas discs (Figs 12 and 13).

(5) In a few cases, the XUV disc is the product of a major merger; for example UGC 04862, identified by Thilker et al. (2007) and UGC 7081, 7651, and 7853, identified by their large FUV concentration. This appears to be an avenue to form some of the type 1 XUV discs.

(6) The H I morphology and anecdotal evidence for small satellite cannibalism all point to a third mechanism for the origin of most XUV discs; cold flow accretion.

With the emergence of new and refurbished radio observatories in preparation for the future Square Kilometre Array (SKA; Carilli & Rawlings 2004), a new window on the 21-cm emission line of atomic hydrogen gas (H I) is opening. The two SKA precursors, the South African Karoo Array Telescope (MeerKAT; Jonas 2007; Booth et al. 2009; de Blok et al. 2009), and the Australian SKA Pathfinder (ASKAP; Johnston 2007; Johnston et al. 2007, 2008a,b; Johnston, Feain & Gupta 2009) stand poised to observe a large number of Southern Hemisphere galaxies in H I in the nearby Universe ($z < 0.2$). In addition, the Extended Very Large Array (EVLA; Napier 2006) and the APERture Tile In Focus instrument (APERTIF; Verheijen et al. 2008; Oosterloo et al. 2009) on the Westerbork Synthesis Radio Telescope (WSRT) will do the same for the Northern Hemisphere. The surveys conducted with these new and refurbished facilities will add new, high-resolution, H I observations on many thousands of galaxies. In the case of WALLABY (Koribalski et al., in preparation), these will be of similar quality spatial resolution as the WHISP survey.

Combining these with existing UV observations from *GALEX*, we can explore the relation between the morphology of the atomic hydrogen and ultraviolet light for much greater samples and in much greater detail. An application of the asymmetry–M_{20} identification of XUV discs in the *GALEX* Nearby Galaxy Atlas (Gil de Paz et al. 2007a) or a sample similar to Lemonias et al. (2011) could reveal additional examples but the combination with deep H I observations can prove the link with cold flows for the majority of XUV discs.

ACKNOWLEDGMENTS

The authors would like to thank D. Thilker for discussions at the Cloister See-On conference, the audience at Leiden Observatory for encouragement for this work and the anonymous referee for his or her comments that improved the science and writing of this paper. The authors acknowledge the use of the HyperLeda data base http://leda.univ-lyon1.fr, the NASA/IPAC Extragalactic Database (NED) which is operated by the Jet Propulsion Laboratory, California Institute of Technology, under contract with the National Aeronautics and Space Administration, and the Westerborg on the Web (WoW) project (http://www.astron.nl/wow/).

The Westerbork Synthesis Radio Telescope is operated by the Netherlands Institute for Radio Astronomy ASTRON, with support of NWO. Based on observations made with the NASA Galaxy Evolution Explorer. GALEX is operated for NASA by the California Institute of Technology under NASA contract NAS5-98034.

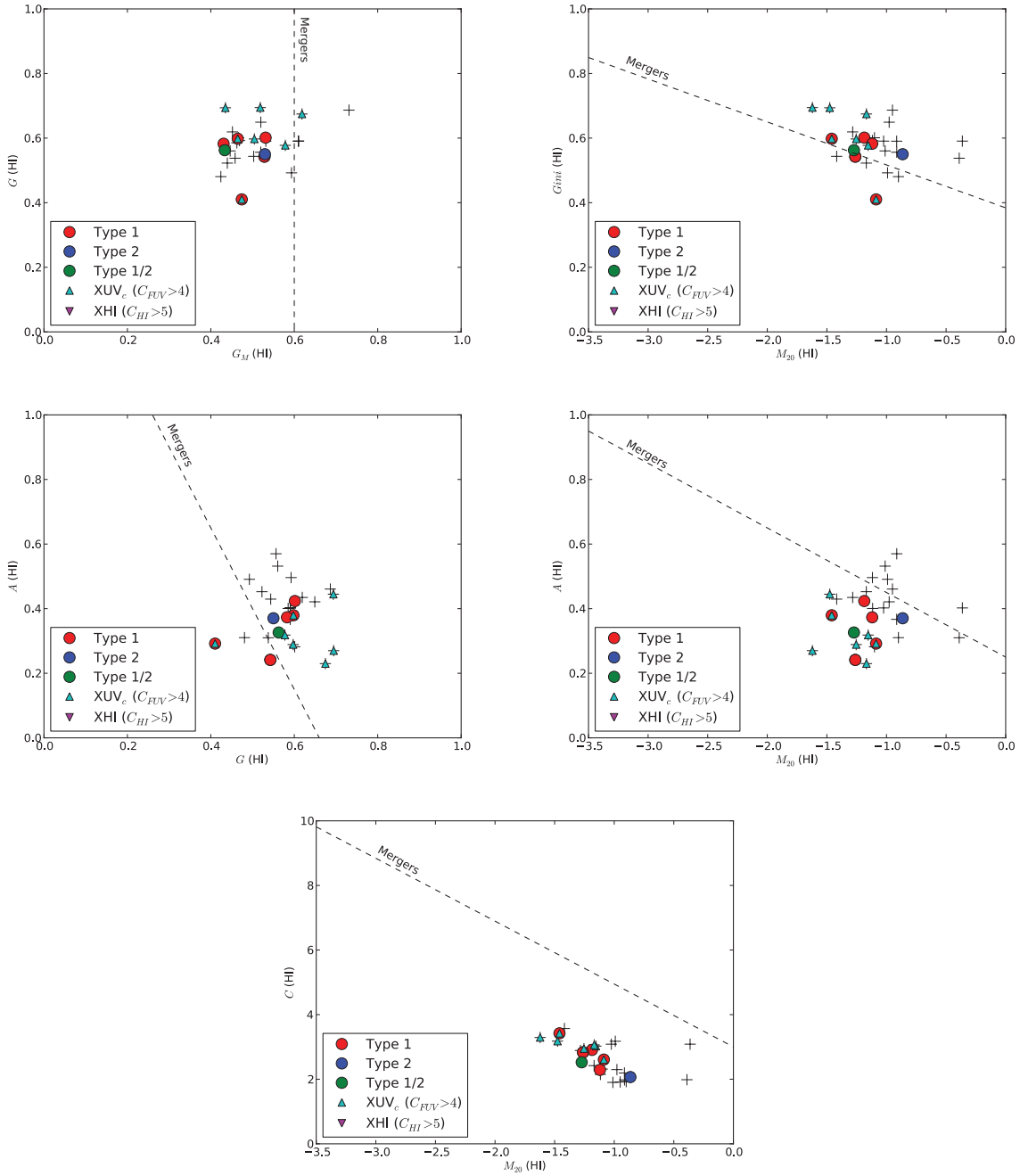

Figure 13. The morphological selection criteria (dashed lines) for H I applied to the THINGS sample. XUV discs identified either by Thilker et al. or via their concentration are marked.

REFERENCES

Alberts S. et al., 2011, ApJ, 731, 28

Allen R. J., 2002, in Taylor A. R., Landecker T. L., Willis A. G., eds, ASP Conf. Ser. Vol. 276, Seeing Through the Dust: The Detection of HI and the Exploration of the ISM in Galaxies. Astron. Soc. Pac., San Francisco, p. 288

Allen R. J., Knapen J. H., Bohlin R., Stecher T. P., 1997, ApJ, 487, 171

Allen R. J., Heaton H. I., Kaufman M. J., 2004, ApJ, 608, 314

Begeman K. G., 1989, A&A, 223, 47

Bertin E., Arnouts S., 1996, A&AS, 117, 393, provided by the NASA Astrophysics Data System

Bigiel F., Leroy A., Walter F., Brinks E., de Blok W. J. G., Madore B., Thornley M. D., 2008, AJ, 136, 2846

Bigiel F., Leroy A., Seibert M., Walter F., Blitz L., Thilker D., Madore B., 2010a, ApJ, 720, L31

Bigiel F. et al., 2010b, ApJ, 725, 1159

Boomsma R., Oosterloo T. A., Fraternali F., van der Hulst J. M., Sancisi R., 2008, A&A, 490, 555

Booth R. S., de Blok W. J. G., Jonas J. L., Fanaroff B., 2009, preprint (arXiv:0910.2935)

Bresolin F., Ryan-Weber E., Kennicutt R. C., Goddard Q., 2009, ApJ, 695, 580

Carilli C. L., Rawlings S., 2004, New A Rev., 48, 979

Conselice C. J., 2003, ApJS, 147, 1

Cuillandre J., Lequeux J., Allen R. J., Mellier Y., Bertin E., 2001, ApJ, 554, 190

de Blok W. J. G., Jonas J., Fanaroff B., Holwerda B. W., Bouchard A., Blyth S., van der Heyden K., Pirzkal N., 2009, in Panoramic Radio Astronomy:

Wide field 1-2 GHz Research on Galaxy Evolution. Proceedings of Science (http://pos.sissa.it/cgi-bin/reader/conf.cgi?confid=89)
Dong H., Calzetti D., Regan M., Thilker D., Bianchi L., Meurer G. R., Walter F., 2008, AJ, 136, 479
Elson E. C., de Blok W. J. G., Kraan-Korteweg R. C., 2011, MNRAS, 415, 323
Ferguson A. M. N., Wyse R. F. G., Gallagher J. S., Hunter D. A., 1998, ApJ, 506, L19
Gil de Paz A. et al., 2005, ApJ, 627, L29
Gil de Paz A. et al., 2007a, ApJS, 173, 185
Gil de Paz A. et al., 2007b, ApJ, 661, 115
Gogarten S. M. et al., 2009, ApJ, 691, 115
Heald G., Allan J., Zschaechner L., Kamphuis P., Rand R., Józsa G., Gentile G., 2011a, in Carignan C., Combes F., Freeman K. C., eds, IAU Symp. 277, Tracing the Ancestry of Galaxies: On the Land of Our Ancestors. Cambridge Univ. Press, Cambridge, p. 59
Heald G. et al., 2011b, A&A, 526, A118
Heiner J. S., Allen R. J., Emonts B. H. C., van der Kruit P. C., 2008a, ApJ, 673, 798
Heiner J. S., Allen R. J., Wong O. I., van der Kruit P. C., 2008b, A&A, 489, 533
Heiner J. S., Allen R. J., van der Kruit P. C., 2009, in The Evolving ISM in the Milky Way and Nearby Galaxies
Heiner J. S., Allen R. J., van der Kruit P. C., 2010, ApJ, 719, 1244
Holwerda B. W., 2005, preprint (astro-ph/0512139)
Holwerda B. W., Pirzkal N., Cox T. J., de Blok W. J. G., Weniger J., Bouchard A., Blyth S.-L., van der Heyden K. J., 2011a, MNRAS, 416, 2426
Holwerda B. W., Pirzkal N., de Blok W. J. G., Bouchard A., Blyth S.-L., van der Heyden K. J., 2011b, MNRAS, 416, 2437
Holwerda B. W., Pirzkal N., de Blok W. J. G., Bouchard A., Blyth S.-L., van der Heyden K. J., Elson E. C., 2011c, MNRAS, 416, 2401
Holwerda B. W., Pirzkal N., de Blok W. J. G., Bouchard A., Blyth S.-L., van der Heyden K. J., Elson E. C., 2011d, MNRAS, 416, 2415
Holwerda B. W., Pirzkal N., de Blok W. J. G., van Driel W., 2011e, MNRAS, 416, 2447
Johnston S., 2007, in From Planets to Dark Energy: the Modern Radio Universe. Proceedings of Science (http://pos.sissa.it/cgi-bin/reader/conf.cgi?confid=52, id. 6)
Johnston S., Feain I. J., Gupta N., 2009, in Saikia D. J., Green D. A., Gupta Y., Venturi T., eds, ASP Conf. Ser. Vol. 407, The Low-Frequency Radio Universe. Astron. Soc. Pac., San Francisco, p. 446
Johnston S. et al., 2007, Publications of the Astronomical Society of Australia, 24, 174
Johnston S. et al., 2008a, Experimental Astronomy, 22, 151
Johnston S. et al., 2008b, Experimental Astronomy, 22, 151
Jonas J., 2007, in From Planets to Dark Energy: the Modern Radio Universe. Proceedings of Science (http://pos.sissa.it/cgi-bin/reader/conf.cgi?confid=52, id. 7)
Kennicutt R. C., Jr, 1998, ApJ, 498, 541
Kereš D., Katz N., Weinberg D. H., Davé R., 2005, MNRAS, 363, 2
Kleinmann S. G. et al., 1994, Exp. Astron, 3, 65
Lelièvre M., Roy J.-R., 2000, AJ, 120, 1306
Lemonias J. J. et al., 2011, ApJ, 733, 74
Lotz J. M., Primack J., Madau P., 2004, AJ, 128, 163
Martínez-Delgado D. et al., 2010, AJ, 140, 962
Martin D. C. et al., 2005, ApJ, 619, L1
Meurer G. R., Carignan C., Beaulieu S. F., Freeman K. C., 1996, AJ, 111, 1551
Meurer G. R., Staveley-Smith L., Killeen N. E. B., 1998, MNRAS, 300, 705
Meurer G. R. et al., 2009, ApJ, 695, 765
Moffett A. J., Kannappan S. J., Baker A. J., Laine S., 2012, ApJ, 745, 34
Muñoz-Mateos J. C. et al., 2009, ApJ, 703, 1569
Napier P. J., 2006, in Backer D. C., Moran J. M., Turner J. L., eds, ASP Conf. Ser. Vol. 356, Revealing the Molecular Universe: One Antenna is Never Enough. Astron. Soc. Pac., San Francisco, p. 65
Nilson P., 1973, Uppsala general catalogue of galaxies. Acta Universitatis Upsaliensis. Nova Acta Regiae Societatis Scientiarum Upsaliensis - Uppsala Astronomiska Observatoriums Annaler, Uppsala: Astronomiska Observatorium
Noordermeer E., van der Hulst J. M., Sancisi R., Swaters R. A., van Albada T. S., 2005a, A&A, 442, 137
Noordermeer E., van der Hulst J. M., Sancisi R., Swaters R. A., van Albada T. S., 2005b, A&A, 442, 137
Oosterloo T., Verheijen M., van Cappellen W., Bakker L., Heald G., Ivashina M., 2009, Proceedings of Wide Field Astronomy & Technology for the Square Kilometre Array (SKADS 2009). Proceedings of Science (http://pos.sissa.it/cgi-bin/reader/conf.cgi?confid=132, id. 70)
Roškar R., Debattista V. P., Brooks A. M., Quinn T. R., Brook C. B., Governato F., Dalcanton J. J., Wadsley J., 2010, MNRAS, 408, 783
Sancisi R., Fraternali F., Oosterloo T., van der Hulst T., 2008, A&A Rev., 15, 189
Scarlata C. et al., 2007, ApJS, 172, 406
Swaters R. A., Balcells M., 2002, A&A, 390, 863
Swaters R. A., van Albada T. S., van der Hulst J. M., Sancisi R., 2002a, A&A, 390, 829
Swaters R. A., van Albada T. S., van der Hulst J. M., Sancisi R., 2002b, A&A, 390, 829
Thilker D. A. et al., 2005a, ApJ, 619, L79
Thilker D. A. et al., 2005b, ApJ, 619, L67
Thilker D. A. et al., 2007, ApJS, 173, 538
Torres-Flores S., Mendes de Oliveira C., de Mello D. F., Scarano S., Jr, Urrutia-Viscarra F., 2012, MNRAS, 421, 3612
van der Hulst J. M., 2002, in Taylor A. R., Landecker T. L., Willis A. G., eds, ASP Conf. Ser. Vol. 276, Seeing Through the Dust: The Detection of HI and the Exploration of the ISM in Galaxies. Astron. Soc. Pac., San Francisco, p. 84
van der Hulst J. M., van Albada T. S., Sancisi R., 2001, in Hibbard J. E., Rupen M., van Gorkom J. H., eds, ASP Conf. Ser. Vol. 240, Gas and Galaxy Evolution. Astron. Soc. Pac., San Francisco, p. 451
Verheijen M. A. W., Oosterloo T. A., van Cappellen W. A., Bakker L., Ivashina M. V., van der Hulst J. M., 2008, in Minchin R., Momjian E., eds, AIP Conf. Ser. Vol. 1035, The Evolution of Galaxies Through the Neutral Hydrogen Window. Am. Inst. Phys., Melville, NY, p. 265
Walter F., Brinks E., de Blok W. J. G., Bigiel F., Kennicutt R. C., Thornley M. D., Leroy A., 2008, AJ, 136, 2563
Werk J. K., Putman M. E., Meurer G. R., Thilker D. A., Allen R. J., Bland-Hawthorn J., Kravtsov A., Freeman K., 2010, ApJ, 715, 656
Zaritsky D., Christlein D., 2007, AJ, 134, 135
Zschaechner L. K., Rand R. J., Heald G. H., Gentile G., Kamphuis P., 2011, ApJ, 740, 35
Zwaan M. A., van der Hulst J. M., Briggs F. H., Verheijen M. A. W., Ryan-Weber E. V., 2005, MNRAS, 364, 1467

APPENDIX A: THE XUV AND XHI DISCS SELECTED BY AUTOMATED MORPHOLOGY

Table A1. The WHISP galaxies identified by their FUV M_{20}-A relation. This is a sample of the full table, which is available as Supporting Information with the online version of the article.

UGC	Thilker et al. 2007 XUV classification
79	–
89	–
94	–
508	–
655	–
718	–
1256	–
1501	–
1913	0
2082	–
2193	–
...	...

APPENDIX C: TABLES OF MORPHOLOGICAL VALUES IN FUV AND NUV

Table C1. The values of the morphological parameters in the H I maps, regridded and scaled to the *GALEX* pixel scale. This is a sample of the full table, which is available as Supporting Information with the online version of the article. (1) UGC catalogue number, (2) the Gini parameter, (3) the M_{20} parameter, (4) concentration, (5) smoothness, (6), ellipticity, (7) G_M, (8) half-light radius.

UGC	Gini	M_{20}	C	A	S	E	G_M	R_{50} (')
00079	0.989 ± 0.000	-1.442 ± 0.048	2.307 ± 0.034	0.719 ± 0.041	0.056 ± 0.002	0.066 ± 0.004	0.982 ± 0.000	0.78
00089	0.974 ± 0.000	-0.704 ± 0.003	5.700 ± 0.015	1.373 ± 0.018	0.045 ± 0.001	0.844 ± 0.000	0.984 ± 0.000	8.4
00094	0.972 ± 0.000	-0.735 ± 0.008	5.839 ± 0.022	1.150 ± 0.028	0.046 ± 0.002	0.843 ± 0.000	0.984 ± 0.000	2.1
00192	0.667 ± 0.000	-1.326 ± 0.007	2.365 ± 0.013	1.037 ± 0.004	0.087 ± 0.000	0.190 ± 0.001	0.603 ± 0.000	4.6
00232	0.982 ± 0.000	-1.597 ± 0.032	2.318 ± 0.033	0.573 ± 0.028	0.050 ± 0.003	0.082 ± 0.005	0.970 ± 0.000	1.0
...								

Table C2. The values of the morphological parameters in the NUV images, smoothed to the WHISP resolution. This is a sample of the full table, which is available as Supporting Information with the online version of the article. Column are the same as in Table C1.

UGC	Gini	M_{20}	C	A	S	E	G_M	R_{50} (')
00079	0.151 ± 0.000	-0.696 ± 0.042	1.508 ± 0.111	0.294 ± 0.021	0.067 ± 0.002	0.004 ± 0.025	0.391 ± 0.000	9.0
00089	0.194 ± 0.001	-0.783 ± 0.030	1.563 ± 0.122	0.372 ± 0.019	0.070 ± 0.002	0.025 ± 0.042	0.402 ± 0.000	8.9
00094	0.193 ± 0.001	-0.810 ± 0.034	1.614 ± 0.128	0.363 ± 0.017	0.071 ± 0.002	0.035 ± 0.030	0.394 ± 0.000	8.9
00192	nan ± ...	0.000 ± 0.000	0.000 ± 0.000	...± ...	...± ...	...± ...	...± ...	15.9
00232	0.299 ± 0.000	-0.745 ± 0.023	1.514 ± 0.094	0.606 ± 0.012	0.170 ± 0.001	0.008 ± 0.022	0.453 ± 0.000	8.9
...								

Table C3. The values of the morphological parameters in the FUV images, smoothed to the WHISP resolution. This is a sample of the full table, which is available as Supporting Information with the online version of the article. Column are the same as in Table C1.

UGC	Gini	M_{20}	C	A	S	E	G_M	R_{50} (')
00079	0.225 ± 0.005	-0.674 ± 0.010	1.386 ± 0.045	0.446 ± 0.013	0.065 ± 0.006	0.124 ± 0.011	0.478 ± 0.000	9.5
00089	0.233 ± 0.006	-0.677 ± 0.011	1.570 ± 0.039	0.452 ± 0.021	0.072 ± 0.010	0.099 ± 0.019	0.475 ± 0.000	9.2
00094	0.197 ± 0.003	-0.782 ± 0.007	1.551 ± 0.054	0.394 ± 0.014	0.065 ± 0.003	0.048 ± 0.014	0.421 ± 0.000	8.9
00192	...± ...	0.000 ± 0.000	0.000 ± 0.000	...± ...	...± ...	...± ...	...± ...	15.9
00232	0.275 ± 0.006	-0.824 ± 0.016	1.608 ± 0.041	0.557 ± 0.021	0.096 ± 0.009	0.056 ± 0.013	0.453 ± 0.000	8.6
...								

SUPPORTING INFORMATION

Additional Supporting Information may be found in the online version of this article:

Appendix A. The XUV and XHI discs selected by concentration.
Appendix B. Distributions of morphological parameters for FUV, NUV and H I.
Appendix C. Tables of morphological values in FUV and NUV.
Appendix D. WHISP galaxies.

Please note: Wiley-Blackwell are not responsible for the content or functionality of any supporting materials supplied by the authors. Any queries (other than missing material) should be directed to the corresponding author for the article.

This paper has been typeset from a TEX/LATEX file prepared by the author.